

# Mechanical behavior and cell response of PCL coated $\alpha$ -TCP foam for cancellous-type bone replacement

Le Thi Bang<sup>a,b</sup>, Kanji Tsuru<sup>b</sup>, Melvin Munar<sup>b</sup>, Kunio Ishikawa<sup>b</sup>, Radzali Othman<sup>a,\*</sup>

<sup>a</sup>*School of Materials and Mineral Resources Engineering, University Sains Malaysia, 14300 Nibong Tebal, Penang, Malaysia*

<sup>b</sup>*Department of Biomaterials, Faculty of Dental Science, Kyushu University, Japan*

Received 2 December 2012; received in revised form 21 December 2012; accepted 21 December 2012

Available online 17 January 2013

## Abstract

The mechanical behavior and cell responses of poly ( $\epsilon$ -caprolactone) (PCL) coated  $\alpha$ -tricalcium phosphate ( $\alpha$ -TCP) foam were studied as an initial step for the fabrication of a cancellous-type artificial bone replacement. The  $\alpha$ -TCP foam was obtained from sintering  $\text{CaCO}_3$  and  $\text{CaHPO}_4 \cdot 2\text{H}_2\text{O}$  at 1500 °C. It was then coated with PCL and its three dimensional fully-interconnected porous structure was found to be maintained. The coated  $\alpha$ -TCP samples exhibited high porosity (80–85%) with large pore size (500–700  $\mu\text{m}$ ) that mimic the cancellous bone structure. The PCL content of the coating layer increased from  $9.3 \pm 0.4 \text{ wt\%}$  to  $19.0 \pm 1.3 \text{ wt\%}$  when coated with 5 wt% to 15 wt% PCL. The compressive strength improved significantly upon PCL coating. The compressive strength of  $\alpha$ -TCP foam,  $30 \pm 10 \text{ kPa}$ , increased to  $750 \pm 20 \text{ kPa}$  when coated with 15 wt% of PCL solution. The in vitro biological evaluations indicated that MC3T3-E1 cells adhered and proliferated well on both the  $\alpha$ -TCP and the PCL coated  $\alpha$ -TCP foams. It was concluded that  $\alpha$ -TCP foam upon coating with bioresorbable PCL is of good potential to fabricate cancellous-type artificial bone replacement.

© 2013 Elsevier Ltd and Techna Group S.r.l. All rights reserved.

**Keywords:** A. Sintering; B. Porosity; C. Mechanical properties; E. Biomedical applications; Tricalcium phosphate

## 1. Introduction

Porous calcium phosphate ceramics have received considerable attention as artificial bone substitutes because of their excellent tissue compatibility and osteoconductivity [1,2]. Open porosity or interconnectivity is especially important for the cells and tissue to penetrate the interior of the porous calcium phosphate. Interconnected pores will be used as the pathways for the transportation of biofluids, nutrients and metabolic wastes [1,3,4]. Among many porous calcium phosphates, calcium phosphate foam gained much attention since it has a fully interconnected porous structure similar to that of cancellous bone and high porosity of more than 80% porosity. Up to date, hydroxyapatite (HAp:  $\text{Ca}_{10}(\text{PO}_4)_6(\text{OH})_2$ ) foam, alpha tricalcium phosphate ( $\alpha$ -TCP) foam, carbonate apatite ( $\text{CO}_3\text{Ap}$ ) foam, and biphasic calcium phosphate foam are the calcium phosphate foams reported and studied [5–8].

Although fully interconnected porous structure and large porosity are ideal from a biological point of view, the porosity and structural architecture of porous CaPs significantly affect their mechanical properties, where the strength decreases when the porosity increases [9,10]. Inherently, natural bone is made up of a biological mineral of CaP and about 40 wt% of bioorganic polymers (mainly collagen type I) [11], which is accountable for the superior strength and partial elasticity in biological tissues [12]. Moreover, composites made from polymers and inorganic components (bioglass/glass–ceramics) had taken advantage of this combination [13,14]. Therefore, the consequent strategy is to combine polymers and CaPs to fabricate scaffolds that meet the requirements desired for bone applications.

It had been shown that the mechanical properties of a ceramic material can be strengthened by the incorporation of a ductile polymer [3,15]. Coating a polymer on a porous CaP is an easy method to produce scaffolds with good mechanical strength whilst maintaining high porosity and large pore size. For example, poly (lactic-co-glycolic) acid (PLGA) coating on  $\text{CO}_3\text{Ap}$  foam was reported to be effective in improving

\*Corresponding author. Tel.: +60 45996122; fax: +60 45941011.

E-mail address: [radzali@eng.usm.my](mailto:radzali@eng.usm.my) (R. Othman).

the mechanical properties of CO<sub>3</sub>Ap foam [16]. However, the fabrication of CO<sub>3</sub>Ap foam is complex since CO<sub>3</sub>Ap is unstable at the high temperatures required for the sintering process. In contrast,  $\alpha$ -TCP is stable at high temperatures and it is also a biodegradable calcium phosphate. Zhao et al. [17] found that the compressive strength of PCL coated porous HA scaffold increased from 0.09 MPa to 0.51 MPa at 20% PCL concentration. However, some macropores might be clogged after coating due to a relatively high PCL concentration being used. Kang et al. [3] attempted to coat the surface of macroporous HA/TCP with a layer of PLGA. Their results indicated that, whilst the coating improved the mechanical properties and retained the biocompatibility of the scaffold, the pore size was much smaller compared to those of cancellous bone.

In this study, therefore,  $\alpha$ -tricalcium phosphate ( $\alpha$ -TCP) foam obtained from CaCO<sub>3</sub> and CaHPO<sub>4</sub>·2H<sub>2</sub>O was coated with poly ( $\epsilon$ -caprolactone) (PCL) to enhance the mechanical properties but maintain the fully interconnected structure as well as a large pore size. The mechanical properties and MC3T3-E1 cell studies of the foams were evaluated as an initial step for the fabrication of a cancellous type artificial bone replacement.

## 2. Materials and method

### 2.1. Fabrication of $\alpha$ -TCP foam

Calcium carbonate (CaCO<sub>3</sub>) (Wako, Osaka, Japan) and dicalcium phosphate dihydrate (CaHPO<sub>4</sub>·2H<sub>2</sub>O) (Wako) powders were mixed in 5 wt% polyvinyl alcohol (Wako) aqueous solution at a Ca/P molar ratio of 1.5 and a powder/liquid ratio of 10/8 (wt/vol). Polyurethane foam templates (HR-20D, Bridgestone, Tokyo, Japan) with approximately 1 mm pore diameter were cut to the appropriate dimensions and dipped into the slurry. The polyurethane foam blocks impregnated with the slurry were then squeezed to remove the excess slurry. After drying at 60 °C for 1 day, the polyurethane foams coated with the powders were fired in air in an electric furnace (SBV-1515D, Motoyama, Osaka, Japan) using a four-stage schedule: (i) heating from room temperature to 400 °C at a heating rate of 1 °C/min to burn out the polyurethane foam and prevent thermal shock; (ii) further heating from 400 °C to 1500 °C at 5 °C/min to allow the sintering reaction between the two chemicals; (iii) a hold at 1500 °C for 5 h to complete sintering, and (iv) cooling down to room temperature in the furnace.

### 2.2. PCL coating on $\alpha$ -TCP foam

5, 10 and 15 wt% PCL solutions were prepared by dissolving PCL (Mn=80,000, Wako) in tetrahydrofuran (THF, Wako). The  $\alpha$ -TCP foams were then dipped into the PCL solution, followed by vacuum infiltration for 5 min. The excess solution was removed by centrifuge (60 rpm) and by blowing compressed air. The PCL coated  $\alpha$ -TCP

foams were dried in a vacuum oven (AVO-200 N; As One, Osaka, Japan) at 37 °C for 5 days to remove any residual solvent. The concentration of PCL solution used for the coating of  $\alpha$ -TCP foam was stated in the parenthesis. For example,  $\alpha$ -TCP foam coated with 5 wt% PCL solution was abbreviated as  $\alpha$ -TCP (5).

### 2.3. Characterization of specimens

The macrostructure of  $\alpha$ -TCP foam specimens before and after PCL coating was observed using an optical microscope (LG-PS2, Olympus, Tokyo, Japan). The microstructure, cross-section and fracture surface were characterized by scanning electron microscopy (SEM: S-3400N, Hitachi High-Technologies Co., Tokyo, Japan). For the SEM observation, the specimens were sputter coated with gold and observed under an accelerating voltage of 10 KV. The PCL content of the PCL coated  $\alpha$ -TCP foam was determined by taking the difference in mass of the  $\alpha$ -TCP foam specimens before and after PCL coating and normalizing the result as a weight percentage of PCL coated  $\alpha$ -TCP foam according to

$$\text{PCL content (wt\%)} = \frac{m_a - m_b}{m_a} \times 100 \quad (1)$$

where  $m_b$  and  $m_a$  are the mass of  $\alpha$ -TCP foams before and after PCL coating (g).

The porosity of the specimens was calculated by the following equations [18]:

$$\text{Porosity (\%)} = 1 - \frac{\rho_a}{\rho_b} \times 100 \quad (2)$$

$$\rho_a = \frac{w_d}{l \times d \times h} \quad (3)$$

where,  $\rho_a$  and  $\rho_b$  are apparent and bulk densities (g/cm<sup>3</sup>), respectively;  $w_d$  is the dried weight of specimen;  $l$ ,  $d$ , and  $h$  are the length, width and depth of the specimen (mm), respectively. The bulk density of specimens was measured using a pycnometer.

### 2.4. Mechanical strength of the specimen

The compressive strength was determined by crushing a rectangular specimen using a computer-controlled universal testing machine (AUTOGRAPH, AGS-J, SHIMADZU, Kyoto, Japan) with a cross-head speed of 1 mm/min. Ten identical samples for each sample group were used in the compressive testing. During loading, the applied force was recorded and the compressive strength was determined at the maximum load before densification.

### 2.5. Cell isolation and culture

MC3T3-E1 osteoblast-like cells (Riken Cell Bank, Tokyo, Japan) were cultured in L-glutamine containing alpha-Minimum Essential Media ( $\alpha$ -MEM, GIBCO/Invitrogen, Grand Island, NY, USA) supplemented with 10 vol% fetal bovine serum (FBS, Invitrogen, Carlsbad, CA, USA),

1 vol% penicillin (10,000 units) and streptomycin (10 mg/ml). The cells were maintained at 37 °C under 5% CO<sub>2</sub> in a humidified atmosphere. The medium was changed every 2 days. At the confluence, the adherent cells were passaged and harvested using 0.25% trypsin-EDTA (Trypin; GIBCO, Invitrogen™, NY, USA).

The  $\alpha$ -TCP foam specimens with dimensions of 10 × 10 × 5 (mm<sup>3</sup>) were sterilized by soaking three times in ethanol 70% for 30 min each, and then rinsed three times with phosphate buffer saline (PBS) (–). It was then placed in a culture medium for 24 h prior to cell seeding. Each experiment was performed in quadruple ( $n=4$ ) for each group.

## 2.6. Cell morphology and proliferation

Cell morphology was observed after 4 h of culture. The cells attached to the  $\alpha$ -TCP foams were rinsed gently with PBS and fixed with 3% glutaraldehyde (SIGMA) in sodium phosphate buffer at 4 °C for 2 h. Subsequently, the  $\alpha$ -TCP foams with cells were dehydrated in a graded series of ethanol solutions (50%, 60%, 70%, 80%, 90% and 100%), and then dried in hexamethyldisilazane (HMDS, Wako, Japan). After complete evaporation of the HMDS, the samples were sputtered with a thin gold film and visualized by SEM.

Alamar Blue dye test (AlamarBlue™; BioSource International Inc, Camarillo, CA, USA) was performed to determine cell viability and proliferation. Cells were loaded on  $\alpha$ -TCP foam specimens at a density of 10<sup>4</sup> cell/cm<sup>2</sup>, and cultured for 3, 5, 7 and 9 days. At each time point, the culture medium was replaced by culture medium containing 10% Alamar Blue reagent and the cells were further incubated for 4 h. The resulting 200  $\mu$ l solution was taken

from all wells, placed in a 96-well clear bottom plate and the fluorescence was measured on a plate reader (Tecan infinite M200, Austria GömbH, Gr dig, Austria) using an excitation and emission wavelength of 520 and 590 nm, respectively.

## 2.7. Statistical analysis

The results were statistically analyzed by ANOVA with Scheffe's test at a significant level of 5%.

## 3. Result

### 3.1. Characterization of the $\alpha$ -TCP foam specimens

Fig. 1 summarizes the macroscopic images of the  $\alpha$ -TCP foams before and after PCL coating. All specimens showed fully interconnected porous structure in spite of the presence or absence of the PCL coating, or the different concentrations of PCL solution used for the PCL coating. The pore diameter is in the range of 500–700  $\mu$ m.

The thickness of the struts slightly increased with the PCL solution concentration. This was further supported

Table 1  
Physical and mechanical properties of  $\alpha$ -TCP foam specimens.

Sample	PCL solution concentration (wt/vol%)	PCL deposited on $\alpha$ -TCP foam after coating (%)	Porosity (%)	Compressive strength (kPa)
$\alpha$ -TCP (0)	0	0	91.5 ± 0.4	30 ± 10
$\alpha$ -TCP (5)	5	9.31 ± 0.5	85.1 ± 0.5	535 ± 17
$\alpha$ -TCP (10)	10	13.53 ± 2.23	81.3 ± 0.6	672 ± 21
$\alpha$ -TCP (15)	15	19.03 ± 1.28	79.3 ± 1.2	750 ± 20

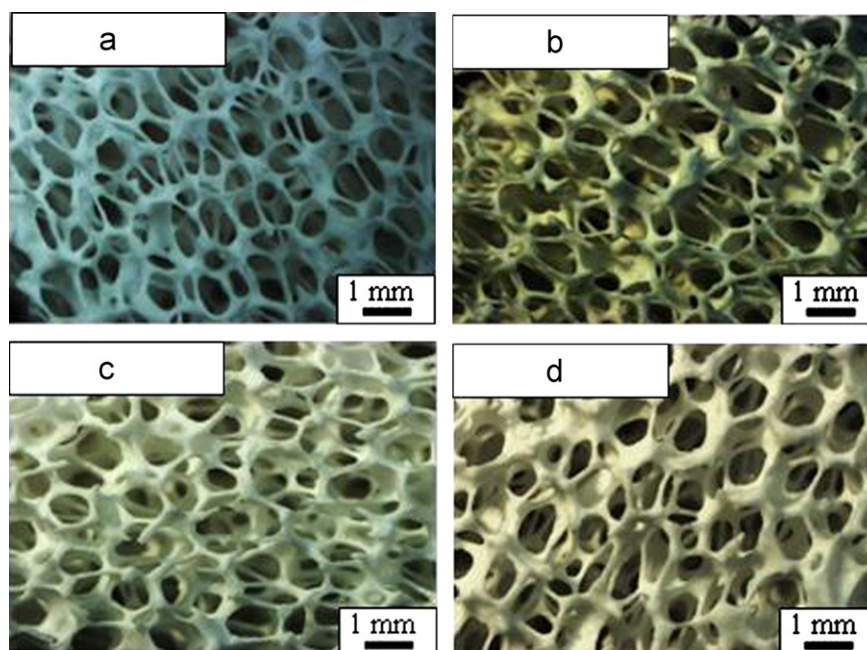


Fig. 1. Optical macrostructure of foam surface. (a)  $\alpha$ -TCP (0), (b)  $\alpha$ -TCP (5), (c)  $\alpha$ -TCP (10) and (d)  $\alpha$ -TCP (15).



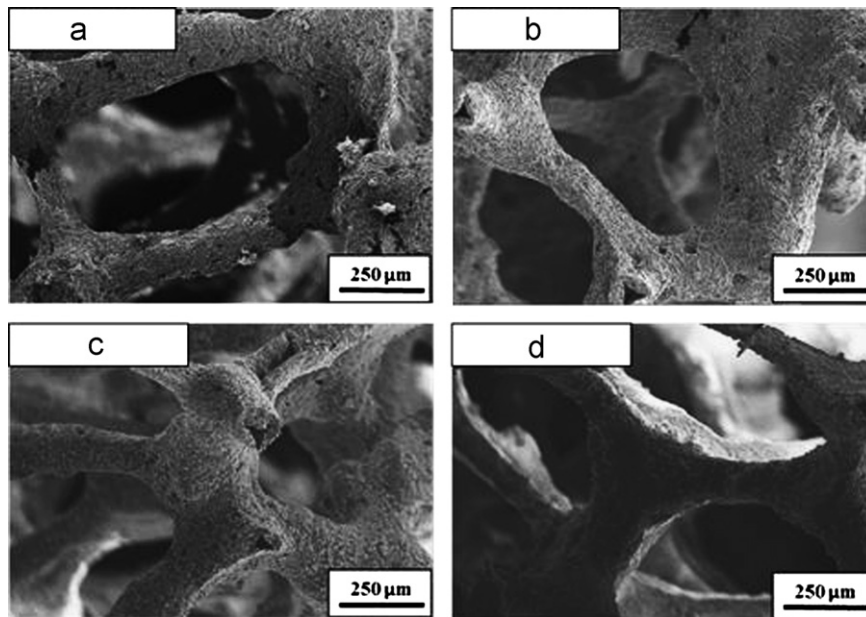


Fig. 2. SEM microstructure images of the  $\alpha$ -TCP foams before and after PCL coating. (a)  $\alpha$ -TCP (0), (b)  $\alpha$ -TCP (5), (c)  $\alpha$ -TCP (10) and (d)  $\alpha$ -TCP (15).

by the PCL content deposited on the  $\alpha$ -TCP foam specimens after coating as shown in Table 1. The PCL content increases with increasing PCL concentration.

The porosity of the  $\alpha$ -TCP foams is also included in Table 1. As shown, the porosity of  $\alpha$ -TCP foam decreases with an increase of the PCL concentration. However, the porosity is still very high even after PCL coating. For example,  $\alpha$ -TCP (15) has  $79.3 \pm 1.2\%$  porosity.

Fig. 2 summarizes the typical SEM images of the  $\alpha$ -TCP foam specimens. The interconnected structure of the  $\alpha$ -TCP foams was also confirmed by the SEM images. The  $\alpha$ -TCP (0) appears with a rough surface whilst the  $\alpha$ -TCP (5),  $\alpha$ -TCP (10) and  $\alpha$ -TCP (15) exhibit a smooth surface morphology indicating that PCL was well embedded on the surface of the struts.

Fig. 3 summarizes a higher magnification of the SEM images. At this magnification, struts of the  $\alpha$ -TCP foam are found to have micropores. In addition, the strut shows a void in the core of the structure. PCL coating is found for  $\alpha$ -TCP (5),  $\alpha$ -TCP (10) and  $\alpha$ -TCP (15). Although partial penetration of PCL was found on the surface of the strut, the micropore of the strut remains unoccupied and the strut keeps the void structure even after the PCL coating.

### 3.2. Compressive strength and fracture surface morphology

Fig. 4 summarizes a typical example of stress–strain curve for  $\alpha$ -TCP (0) and  $\alpha$ -TCP (15). Brittleness is confirmed for  $\alpha$ -TCP (0) foam, which was evidenced by an elastic–brittle manner (Fig. 4(a)). In other words, the  $\alpha$ -TCP (0) foams crushed and disintegrated due to the brittle fracture of the struts. On the other hand, the brittle fracture of the PCL coated  $\alpha$ -TCP exhibits three typical regimes as shown by the stress–strain curve in Fig. 4(b): (i)

a positive slope when a maximum stress is reached, (ii) the maximum stress causes the struts of the foam to fracture in a brittle manner, (iii) compaction of the debris in the presence of PCL as the stress increases.

The compressive strengths of the different  $\alpha$ -TCP foams are shown in Table 1. There is a clear difference between the compressive strength of the  $\alpha$ -TCP foam free from PCL coating and PCL coated  $\alpha$ -TCP foams. Compressive strength of the  $\alpha$ -TCP (0) is  $30 \pm 10$  kPa whereas that of  $\alpha$ -TCP (15) is  $750 \pm 20$  kPa. When the compressive strengths are compared among the PCL coated  $\alpha$ -TCP foams, a higher value is obtained for the  $\alpha$ -TCP coated with a higher concentration of PCL solution.

Fig. 5 summarizes the typical fracture surface morphologies at breaking point. In the case  $\alpha$ -TCP foam free from PCL coating, the struts simply disrupted as shown in Fig. 5 (a). Similarly, the struts also disrupted for the PCL coated  $\alpha$ -TCP foams (Fig. 5 (b), (c), (d)). However, the struts of PCL coated  $\alpha$ -TCP foams exhibit the formation of thin fibrils at the rupture point (Fig. 5(b), (c), (d)). Although the coating layer was stretched, it still remained well-bonded to the ceramic phase.

### 3.3. Cell morphology and proliferation

The morphologies of MC3T3-E1 cells cultured on the surfaces of  $\alpha$ -TCP foams with and without PCL coating for 4 h is shown in Fig. 6. Attached cells on the  $\alpha$ -TCP free from PCL coating and  $\alpha$ -TCP coated PCL have the similar morphologies with flattened and polygonal spread appearance. This result suggested that cells can attach and spread well on both surfaces. Once attached to the surface, cells will grow in number to cover the entire implant surface before initiating differentiation [19] upon further incubation.

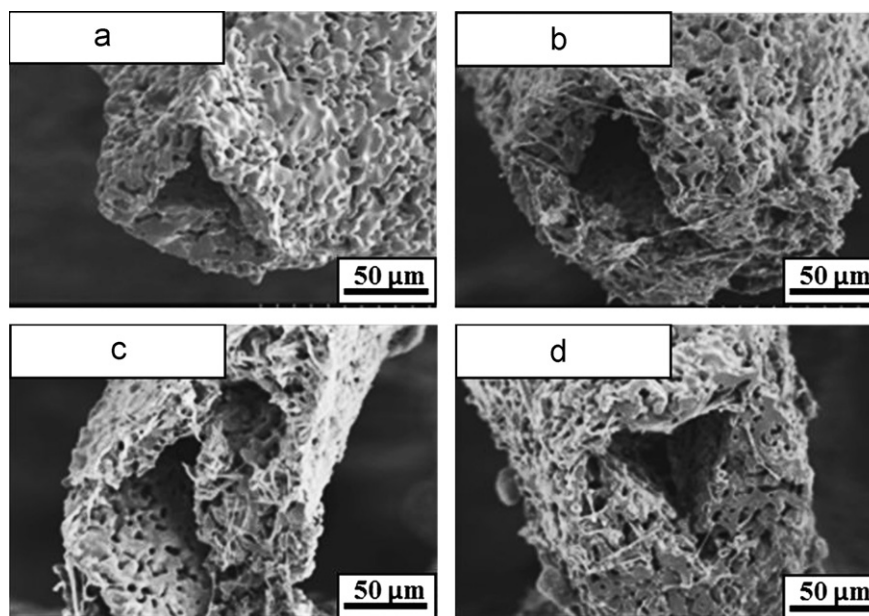


Fig. 3. Cross-section of  $\alpha$ -TCP foam specimens before and after PCL coating. (a)  $\alpha$ -TCP (0), (b)  $\alpha$ -TCP (5), (c)  $\alpha$ -TCP (10) and (d)  $\alpha$ -TCP (15).

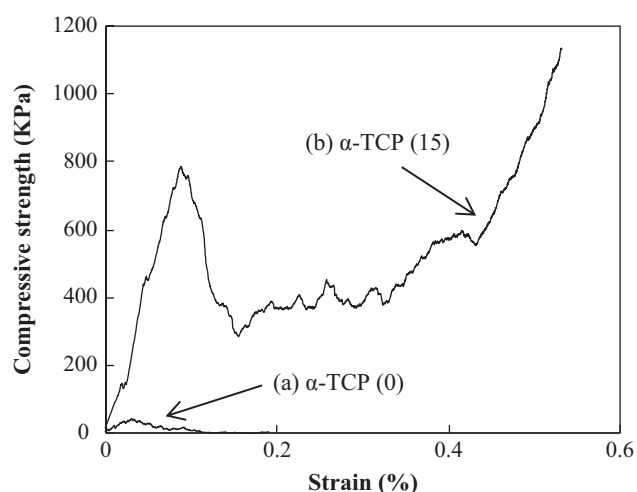


Fig. 4. Typical stress–strain curve of foam specimens upon compression test.

Fig. 7 shows a typical example of proliferation of MC3T3-E1 cells on  $\alpha$ -TCP (0) and  $\alpha$ -TCP (10) over a culture period of 9 days. With incubation time, the cell proliferation on both  $\alpha$ -TCP (0) and  $\alpha$ -TCP (10) increases. This indicates that MC3E3-E1 cells can proliferate well on both  $\alpha$ -TCP and  $\alpha$ -TCP coated PCL foams. After day 5,  $\alpha$ -TCP (0) exhibits the higher increase in cell proliferation compared to  $\alpha$ -TCP (10).

#### 4. Discussion

PCL has been used in biomedical applications because of its excellent tissue compatibility, biodegradability, and non-toxicity [18,20,21], especially in drug delivery devices [22]. The results obtained in the present study demonstrated clearly

that the mechanical properties of  $\alpha$ -TCP foam can be improved significantly by PCL coating. Compressive strength of the foam increased approximately 25 times and the brittle foam became tough upon PCL coating.

The results are in good agreement with previous papers stating that ceramics can be strengthened and toughened by the incorporation of a ductile polymer [3,5,12,13]. However, when polymer was coated on a porous ceramic, the macropores were, in some part, clogged after coating [15,23]. Fortunately, no clogging was observed by the PCL coating of  $\alpha$ -TCP foam. This may due, at least in part, to the fully interconnected porous structure and the very high porosity. The limited PCL concentration is also thought to contribute to the non-clogging behavior since lower PCL concentration results in solution of lower viscosity. The mechanical properties of  $\alpha$ -TCP foam are believed to be increased by the tight adhesion between  $\alpha$ -TCP and PCL. According to Nalla et al. [24], one of the mechanism of toughening in bone was the crack-binding by the collagen fibrils. The fracture surface showed the formation of fibrils which is similar to that of collagen fibrils in cortical bone at the fracture surface [24]. Thus, coating with PCL not only increased the mechanical strength of  $\alpha$ -TCP foam, but also toughened the  $\alpha$ -TCP foam. In fact, our preliminary results indicated that dipping of  $\alpha$ -TCP in PCL solution under vacuum resulted in PCL coated  $\alpha$ -TCP foam with higher mechanical strength when compared with just dipping (data not shown). As shown in Fig. 3, the strut of  $\alpha$ -TCP foam showed microporous structure. Therefore, degassing could be effective for the penetration of PCL into the micropores on the surface of  $\alpha$ -TCP foam struts. Interestingly, no penetration of PCL was found in the voids of the  $\alpha$ -TCP as shown in Fig. 3. Although penetration of PCL into the voids of  $\alpha$ -TCP foam struts may further increase the mechanical properties of  $\alpha$ -TCP foam,

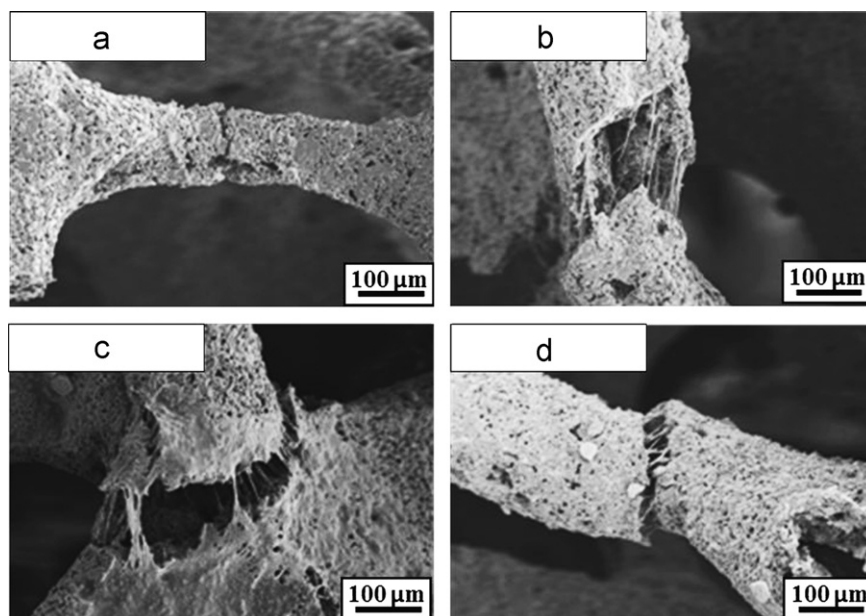


Fig. 5. Typical fracture struts at breaking point of the  $\alpha$ -TCP foams before and after PCL coating. (a)  $\alpha$ -TCP (0), (b)  $\alpha$ -TCP (5), (c)  $\alpha$ -TCP (10) and (d)  $\alpha$ -TCP (15).

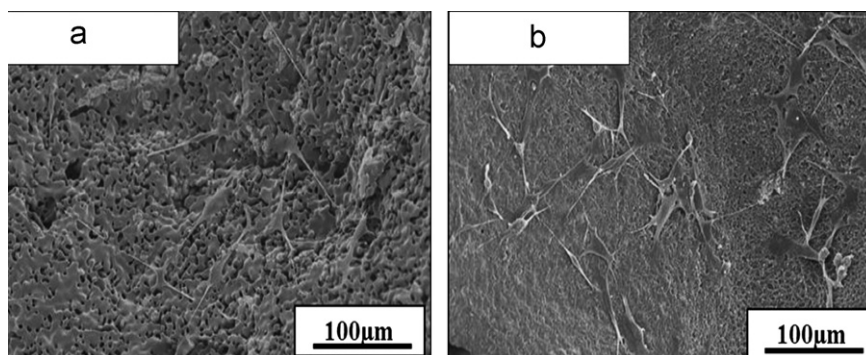


Fig. 6. Cell morphology after culture on the specimens for 4 h. (a)  $\alpha$ -TCP (0) and (b)  $\alpha$ -TCP (5).

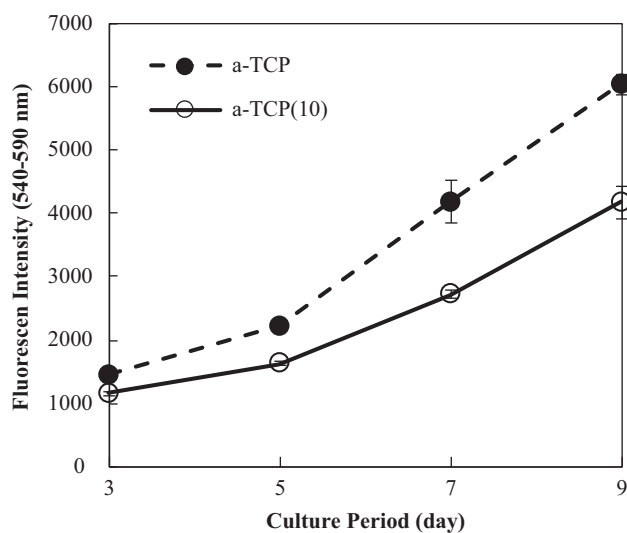


Fig. 7. Proliferation of MC3T3-E1 cells on the different  $\alpha$ -TCP foams after 3, 5, 7 and 9 days in culture.

the voids could be useful for the drug delivery system since drugs may be loaded inside the voids [25,26].

The biocompatibility was investigated through performing MC3T3-E1 cell attachment and proliferation. The results indicated that, there were no differences in cell behavior, in term of cell morphology as shown in Fig. 6. Cells attached on both  $\alpha$ -TCP free from PCL and PCL coated  $\alpha$ -TCP had the filopodia appearance. These filopodia with polygonal shape spreading on the surface of the material increased the contact area with the implant surface [27], and may be useful for tissue ingrowth and bone formation [15] into the porous  $\alpha$ -TCP foams. The cell proliferation increased with the culture period indicating the possibility of improving long term biocompatibility [28] of the  $\alpha$ -TCP foam specimens. Hence, coating with PCL maintained the biological properties in addition to significantly enhancing the mechanical properties of the  $\alpha$ -TCP foam.

However, the proliferation of MC3T3-E1 cells on PCL coated  $\alpha$ -TCP foam was lower than that on the pure  $\alpha$ -TCP,

and so, drawback of the PCL coating may be a possible decrease of osteoconductivity and tissue compatibility. These properties should be evaluated by the histological studies based on the initial results obtained in the present study.

## 5. Conclusions

PCL coating on  $\alpha$ -TCP foam was found to be very effective in increasing the mechanical strength and toughening the  $\alpha$ -TCP foam. The  $\alpha$ -TCP and PCL coated  $\alpha$ -TCP foams exhibited excellent biocompatibility. The compressive strength of the  $\alpha$ -TCP foam increased approximately by 25 times when compared to  $\alpha$ -TCP foam free from PCL. It was concluded that PCL coated  $\alpha$ -TCP foam have a good possibility to be used as artificial bone replacement.

## Acknowledgment

This study was supported in part by a Grant-in-Aid for Scientific Research from the Japan Science and Technology Agency, Ministry of Education, Sports, Culture, Science and Technology, Japan, and by the AUN/SEED-Net project under the Japan International Cooperation Agency (JICA).

## References

- [1] D.W. Huttmacher, Scaffolds in tissue engineering bone and cartilage, *Biomaterials* 21 (2000) 2529–2543.
- [2] K. Rezwan, Q.Z. Chen, J.J. Blaker, A.R. Boccaccini, Biodegradable and bioactive porous polymer/inorganic composite scaffolds for bone tissue engineering, *Biomaterials* 27 (2006) 3413–3431.
- [3] Y. Kang, A. Scully, D.A. Young, S. Kim, H. Tsao, M. Sen, et al., Enhanced mechanical performance and biological evaluation of a PLGA coated  $\beta$ -TCP composite scaffold for load-bearing applications, *European Polymer Journal* 47 (2011) 1569–1577.
- [4] O. Gauthier, E. Goyenvalle, J.M. Bouler, J. Guicheux, P. Pilet, P. Weiss, et al., Macroporous biphasic calcium phosphate ceramics versus injectable bone substitute: a comparative study 3 and 8 weeks after implantation in rabbit bone, *Journal of Materials Science: Materials in Medicine* 12 (2001) 385–390.
- [5] X. Miao, D.M. Tan, J. Li, Y. Xiao, R. Crawford, Mechanical and biological properties of hydroxyapatite/tricalcium phosphate scaffolds coated with poly(lactic-co-glycolic acid), *Acta Biomaterialia* 4 (2008) 638–645.
- [6] M. Munar, U. Koh-ichi, I. Kunio, M. Shigeki, N. Masaharu, Effects of sintering temperature over 1300 °C on the physical and compositional properties of porous hydroxyapatite foam, *Dental Materials Journal* 25 (2006) 51–58.
- [7] A. Takeuchi, M.L. Munar, H. Wakae, M. Maruta, S. Matsuya, K. Tsuru, et al., Effect of temperature on crystallinity of carbonate apatite foam prepared from alpha-tricalcium phosphate by hydrothermal treatment, *Biomedical Materials and Engineering* 19 (2009) 205–211.
- [8] S.I. Roohani-Esfahani, S. Nouri-Khorasani, Z. Lu, R. Appleyard, H. Zreiqat, The influence hydroxyapatite nanoparticle shape and size on the properties of biphasic calcium phosphate scaffolds coated with hydroxyapatite–PCL composites, *Biomaterials* 31 (2010) 5498–5509.
- [9] I. Sopyan, J. Kaur, Preparation and characterization of porous hydroxyapatite through polymeric sponge method, *Ceramics International* 35 (2009) 3161–3168.
- [10] L.-H. He, O.C. Standard, T.T.Y. Huang, B.A. Latella, M.V. Swain, Mechanical behaviour of porous hydroxyapatite, *Acta Biomaterialia* 4 (2008) 577–586.
- [11] F. Sun, H. Zhou, J. Lee, Various preparation methods of highly porous hydroxyapatite/polymer nanoscale biocomposites for bone regeneration, *Acta Biomaterialia* 7 (2011) 3813–3828.
- [12] A.J. Wagoner-Johnson, B.A. Herschler, A review of the mechanical behavior of CaP and CaP/polymer composites for applications in bone replacement and repair, *Acta Biomaterialia* 7 (2011) 16–30.
- [13] L.C. Gerhardt, A.R. Boccaccini, Bioactive glass and glass-ceramic scaffolds for bone tissue engineering, *Materials* 3 (2010) 3867–3910.
- [14] A.R. Boccaccini, J.J. Blaker, V. Maquet, R.M. Day, R. Jérôme, Preparation and characterisation of poly(lactide-co-glycolide) (PLGA) and PLGA/Bioglass® composite tubular foam scaffolds for tissue engineering applications, *Materials Science and Engineering: C* 25 (2005) 23–31.
- [15] J. Zhao, X. Lu, K. Duan, L.Y. Guo, S.B. Zhou, J. Weng, Improving mechanical and biological properties of macroporous HA scaffolds through composite coatings, *Colloids and Surfaces B: Biointerfaces* 74 (2009) 159–166.
- [16] M.M. Girdle, L.M. Melvin, T. Kanji, M. Shigeki, K. Ishikawa, Mechanical strength improvement of carbonate apatite foam bone substitute by PLGA reinforcement, in: *Proceedings of the 6th International Joint Symposium on “Dental and Craniofacial Morphogenesis and Tissue Regeneration” and “Oral Health Science”*, 2011.
- [17] J. Zhao, K. Duan, J.W. Zhang, X. Lu, J. Weng, The influence of polymer concentrations on the structure and mechanical properties of porous polycaprolactone-coated hydroxyapatite scaffolds, *Applied Surface Science* 256 (2010) 4586–4590.
- [18] M. Yeo, H. Lee, G. Kim, Three-dimensional hierarchical composite scaffolds consisting of polycaprolactone,  $\beta$ -tricalcium phosphate, and collagen nanofibers: fabrication, physical properties, and in vitro cell activity for bone tissue regeneration, *Biomacromolecules* 12 (2011) 502–510.
- [19] R. Narayan, A. Bandyopadhyay, S. Bose (Eds.), *Ceramic Transactions*, vol. 228, Wiley, 2011.
- [20] J.R. Porter, A. Henson, K.C. Popat, Biodegradable poly(epsilon-caprolactone) nanowires for bone tissue engineering applications, *Biomaterials* 30 (2009) 780–788.
- [21] E. Jabbari, S. Wang, L. Lu, J.A. Gruetzmacher, S. Ameenuddin, T.E. Hefferan, et al., Synthesis, material properties, and biocompatibility of a novel self-cross-linkable poly(caprolactone fumarate) as an injectable tissue engineering scaffold, *Biomacromolecules* 6 (2005) 2503–2511.
- [22] F. Lu, Y.Y. Shen, Y.Q. Shen, J.W. Hou, Z.M. Wang, S.R. Guo, Treatments of paclitaxel with poly(vinyl pyrrolidone) to improve drug release from poly(epsilon-caprolactone) matrix for film-based stent, *International Journal of Pharmaceutics* 434 (2012) 161–168.
- [23] H.W. Kim, J.C. Knowles, H.E. Kim, Hydroxyapatite/poly(epsilon-caprolactone) composite coatings on hydroxyapatite porous bone scaffold for drug delivery, *Biomaterials* 25 (2004) 1279–1287.
- [24] R.K. Nalla, J.S. Stöken, J.H. Kinney, R.O. Ritchie, Fracture in human cortical bone: local fracture criteria and toughening mechanisms, *Journal of Biomechanics* 38 (2005) 1517–1525.
- [25] H. Wu, S. Zhang, J. Zhang, G. Liu, J. Shi, L. Zhang, et al., A hollow-core, magnetic, and mesoporous double-shell nanostructure: in situ decomposition/reduction synthesis, bioimaging, and drug-delivery properties, *Advanced Functional Materials* 21 (2011) 1850–1862.
- [26] Y. Chen, X. Zheng, H. Qian, Z. Mao, D. Ding, X. Jiang, Hollow core-porous shell structure poly(acrylic acid) nanogels with a super-high capacity of drug loading, *ACS Applied Materials & Interfaces* 2 (2010) 3532–3538.
- [27] I.M. Martínez, L. Meseguer-Olmo, A. Bernabeu-Esclapez, P.A. Velásquez, P.N. De Aza, In vitro behavior of  $\alpha$ -tricalcium phosphate doped with dicalcium silicate in the system  $\text{Ca}_2\text{SiO}_4\text{--Ca}_3(\text{PO}_4)_2$ , *Materials Characterization* 63 (2012) 47–55.
- [28] Y. Zhang, M. Zhang, Cell growth and function on calcium phosphate reinforced chitosan scaffolds, *Journal of Materials Science: Materials in Medicine* 15 (2004) 255–260.